scientific reports

Check for updates

OPEN

TiO_2 nanotube-supported Cu(II)-Schiff base complex as an efficient heterogeneous catalyst for A^3 coupling reactions under solvent-free conditions

Fariba Javan Sharabiani[1], Sahar Baniyaghoob[1]✉, Mojtaba Amini[2]✉ & Ali Akbar Khandar[2]

A novel Cu(II)-Schiff base complex supported on TiO_2 nanotubes was successfully synthesized through a multi-step procedure. The resulting nanocatalyst was characterized using powder X-ray diffraction (XRD), Fourier-transform infrared spectroscopy (FT-IR), field emission scanning electron microscopy (FE-SEM), transmission electron microscopy (TEM), energy-dispersive X-ray spectroscopy (EDX), and X-ray photoelectron spectroscopy (XPS). The catalytic activity of the synthesized material was evaluated in the three-component (A^3) coupling reaction involving aldehydes, amines, and alkynes under solvent-free conditions. The catalyst demonstrated excellent activity, affording good to excellent yields across a range of tested substrates. The optimal reaction conditions were established, and the catalyst's reusability was investigated. However, a leaching test revealed significant Cu species in the solution, suggesting potential homogeneous catalysis. Despite this, the catalyst showed promising recyclability over multiple runs. Further analysis, including ICP-MS or AAS, could be useful to quantify the leached Cu and confirm the catalyst's stability in longer cycles.

Keywords TiO_2 nanotubes, Schiff base complex, Catalyst, A^3 coupling reaction, Propargylamine

The A^3 coupling reaction which refers to the three-component coupling of amines, aldehydes, and terminal alkynes is of fundamental importance in organic synthesis[1]. The coupling products, propargylamine derivatives are key intermediates for synthesis of numerous chemicals including biological and pharmaceutical molecules[2,3]. The term A^3 coupling was used for the first time by Li et al. in 2002 for the synthesis of propargylamine derivatives using transition metal catalysts[4]. Cu(I) salts were the most used catalysts in the early researches; however the efforts in the next years revealed the capability of different transition metal compounds for catalyzing the A^3 coupling reactions[5–9]. A variety of homogeneous and heterogeneous catalysts including metal salts[10,11], metal complexes[12–14], metal nanoparticles (MNPs)[15,16], metal oxide nanoparticles[17–19], and core-shell structures[20–22] have been applied in A^3 coupling reactions.

Among different catalysts examined for A^3 coupling, metal complexes of Schiff bases are considered as promising candidates in last few years. Schiff bases are synthesized by the condensation of amines with carbonyl compounds and contain imine groups (-RC = N-) in their structure. Naeimi and co-workers[23] introduced a thioether-based copper(I)-Schiff base complex as an efficient catalyst for A^3 coupling reaction. According to the results, the thiosalen ligand improved the catalytic activity of copper(I) because of the electron-rich feature of sulfur atoms. The A^3 coupling reactions produced propargylamines as the sole products with high yields (> 80%). Varyani et al.[24] prepared a complex of copper(II) ions with amino acid ionic liquid Schiff base derived from DL-threonine and salicylaldehyde. The complex was tested as a catalyst in A^3 coupling reactions and a maximum conversion of 95% was obtained under optimized conditions using water as a solvent. Agrahari et al.[25] revealed that the heterogeneous catalysis of A^3 coupling reaction by salen-type Cu(II)-Schiff base complex proceeds through a mechanism involving the reversible conversion of Cu(II) to Cu(I).

Despite the excellent performance of aforementioned homogeneous catalysts, their recovery remains a challenge. Numerous efforts have been made to tackle this problem. In this regards, immobilization of

[1]Department of Chemistry, Science and Research Branch, Islamic Azad University, P.O. Box 14515-775, Tehran, Iran. [2]Department of Inorganic Chemistry, Faculty of Chemistry, University of Tabriz, P.O. Box 5166616471, Tabriz, Iran. ✉email: baniyaghoob@srbiau.ac.ir; mojtaba_amini@tabrizu.ac.ir

homogenous catalysts on solid supports was suggested by some authors. Terra et al.[26] achieved high yields of propargylamines by utilizing amine-functionalized MCM-41 as a support for Cu(I) species. Kaur and co-workers[27] developed chitosan-supported copper(I) catalysts for application in A^3 coupling and decarboxylative A^3 coupling reactions. The catalysts benefit from easy recyclability and successive reusability with negligible loss in their activity. Encapsulation of a copper(I)-Schiff base complex with N_2S_2-donor into porous NaY zeolite was reported recently[28]. The immobilized complex was recycled and reused for 8 cycles in A^3 coupling reaction, and the yield was decreased by only about 9% after eighth run.

Herein we decided to use TiO_2 nanotubes (TNTs) as support for immobilizing Cu(II)-Schiff base complex. TiO_2 nanotubes have been attracted immense attention in recent years due to their large surface area, chemical inertness, nontoxicity, large adsorption capacities, and charge transport property[29–32]. While several studies have documented the synthesis of Schiff bases and their metal complexes on TiO_2 nanoparticles[33–36], analogous developments for TiO_2 nanotubes remain notably limited. For stabilizing Schiff base on TNTs, we modified its surface with 3-aminopropyl triethoxy silane (APTES) which provides a chemical junction between TNTs and organic ligand. Subsequent condensation of APTES as an amine with salicylaldehyde and complexation with Cu(II) resulted in an immobilized Cu(II)-Schiff base complex. We also evaluated the catalytic activity of prepared material in three component coupling reactions.

Experimental

Synthesis of TiO_2 nanotubes (TNTs)

TiO_2 nanotubes were synthesized using a straightforward hydrothermal approach. For this purpose, 0.428 g of anatase TiO_2 powder (particle diameter < 0.1 mm) and 0.5 g of sodium dodecyl sulfate (SDS, Merck) were added into 50 mL of a 10 M NaOH solution. The mixture was vigorously stirred for 1 h, followed by sonication for an additional hour to achieve homogeneity. The resulting milky suspension was then transferred into a 100 mL Teflon-lined stainless steel autoclave and heated at 140 °C for 72 h. After cooling, the solid product was aged for 12 h in diluted nitric acid (pH = 2) to enable ionic exchange of Na^+ with H^+. Finally, the white powder was collected by filtration, washed with absolute ethanol and distilled water several times, and dried at 60 °C for 12 h.

Preparation of TNT@APTES

To prepare APTES-grafted TNTs, 1 g of synthesized TNTs was dispersed in 30 mL of toluene (Merck). Subsequently, 2 mL of 3-aminopropyl triethoxy silane (APTES, Sigma-Aldrich) was added dropwise to the dispersion under stirring. The stirring was continued for 24 h at reflux condition to ensure complete grafting. Then, the product was filtered, thoroughly washed with ethanol and water, and dried at room temperature. In this way, TNT@APTES was obtained.

Synthesis of Cu(II)-Schiff base complex on TNTs

In this process, 0.5 g of TNT@APTES (synthesized as described in Sect. 2.2) was added to 50 mL of ethanol and sonicated for 20 min. Next, 3 mmol of salicylaldehyde (Merck) was added to the mixture, and the reaction was allowed to proceed under reflux conditions at 80 °C with continuous stirring for 24 h. The obtained yellow solid was filtered, washed with ethanol and distilled water several times, to completely remove unreacted precursors, and dried at room temperature.

The dried powder was then dispersed in 30 mL of ethanol using ultrasound irradiation. To this suspension, 1.5 mmol of copper(II) acetate (Merck) was added, and the reaction mixture was stirred under reflux condition at 80 °C for 24 h. The green-colored solid product was separated by filtration, washed with excess amounts of ethanol (30 mL) and distilled water (30 mL), and dried at 50 °C for 24 h. The obtained sample was denoted as TNT@Cu(II)-SB.

Characterization

The powder X-ray diffraction (XRD) patterns of synthesized materials were collected by a Tongda TD-3700 diffractometer using Cu kα radiation (λ = 1.5406 Å) in the 2θ range of 7–70 °. Fourier-transform infrared (FT-IR) spectroscopy was performed on a Bruker Tensor 27 spectrometer to investigate the presence of functional groups. Morphological analysis was conducted using scanning electron microscopy (Tescan MIRA3 FE-SEM, operated at 15 kV) and transmission electron microscopy (TEM, the FEI Tecnai 20 instrument). Elemental composition was determined via energy-dispersive X-ray spectroscopy (EDX, operated at an accelerating voltage of 20 kV) integrated with the FE-SEM system.

Catalytic tests

TiO_2 nanotubes-supported Cu(II)-Schiff base complex (TNT@Cu(II)-SB) was tested as a catalyst in A^3 coupling of aldehydes, amines, and alkynes for synthesis of propargylamines. In a typical procedure, 4 mg of catalyst was added to a vial containing aldehyde (0.55 mmol), amine (0.55 mmol) and alkyne (0.5 mmol), and the mixture was magnetically stirred at 120 °C for 4 h under air. After completion, 3 mL of water was added to the reaction mixture, and the product was extracted using ethyl acetate (2 × 10 mL). Finally, the organic solvent was evaporated to afford the corresponding propargylamine without further purification.

Results and discussion

Characterization

To assess the crystallinity of synthesized samples, XRD patterns were provided and are presented in Fig. 1. As can be seen, the XRD pattern of TiO_2 nanopowder used as the precursor shows the characteristic peaks of anatase phase at 2θ = 25.27, 36.87, 37.68, 47.97, 53.78, 55.03, 62.60, and 68.70° corresponding to the (101), (103), (004),

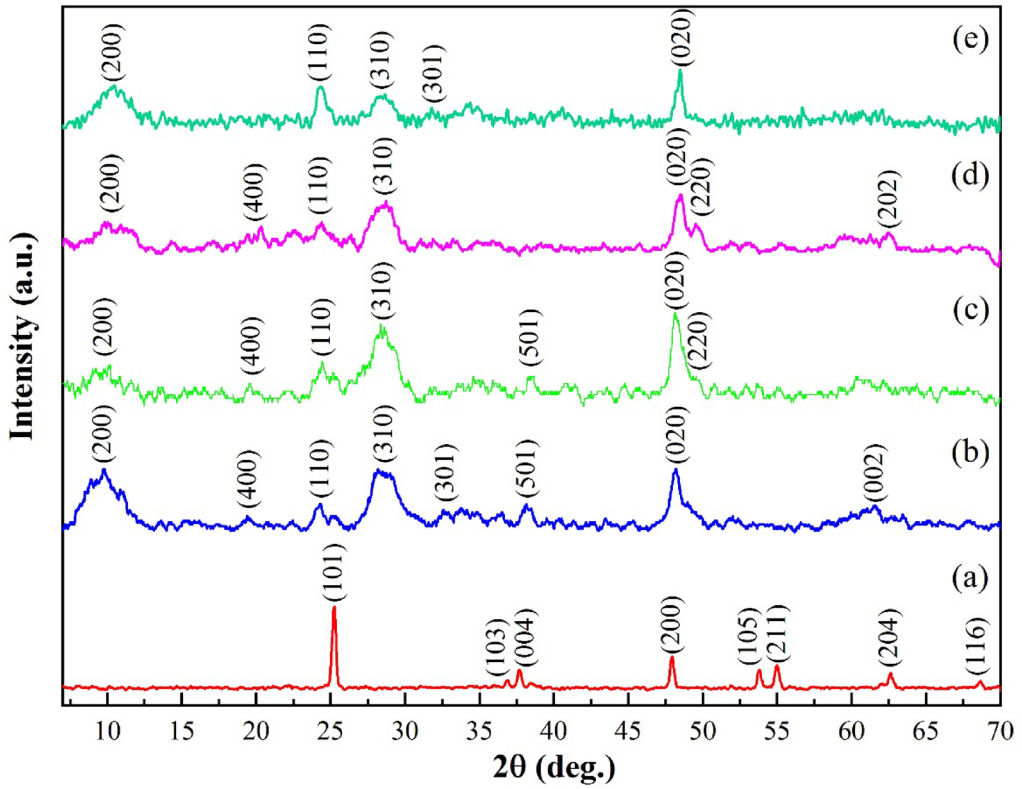

Fig. 1. XRD patterns of (**a**) TiO_2 nanopowder, (**b**) TNTs, (**c**) TNTs@ APTES, (**d**) TNTs@SB, and (**e**) TNTs@ Cu(II)-SB.

(200), (105), (211), (204), and (116) reflection planes, respectively (JCPDS No. 071–1169). After hydrothermal treatment of TiO_2 nanopowder in concentrated NaOH solution, the XRD pattern changes drastically and new peaks appears at 2θ = 9.78, 19.37, 24.29, 27.93, 32.61, 38.09, 48.23, and 61.58°. The observed peaks can be attributed to the (200), (400), (110), (310), (301), (501), (020), and (002) reflection planes of $H_2Ti_2O_5.H_2O$ (JCPDS No. 47–0124), respectively[37]. The low intensity of XRD peaks reveals the poor crystallinity of synthesized TNTs. Moreover, all peaks are broad due to the small size of crystallites[38]. Upon modification of TNTs with APTES (TNTs@APTES), synthesis of Schiff base (TNTs@SB) and preparation of Cu(II)-Schiff base complex

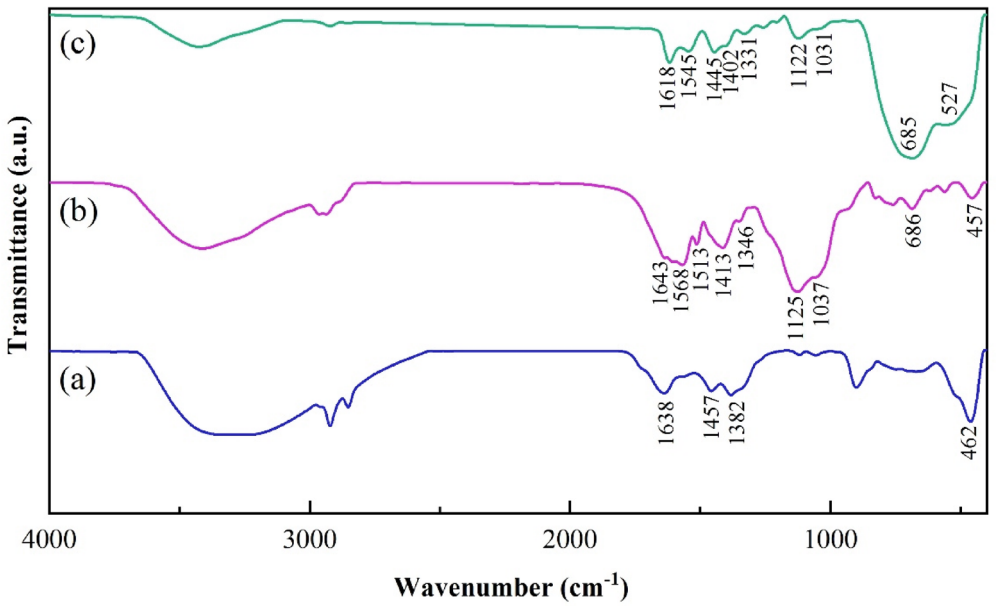

Fig. 2. FT-IR spectra of TNTs (**a**), Cu(II)-SB complex (**b**), and TNTs@Cu(II)-SB (**c**).

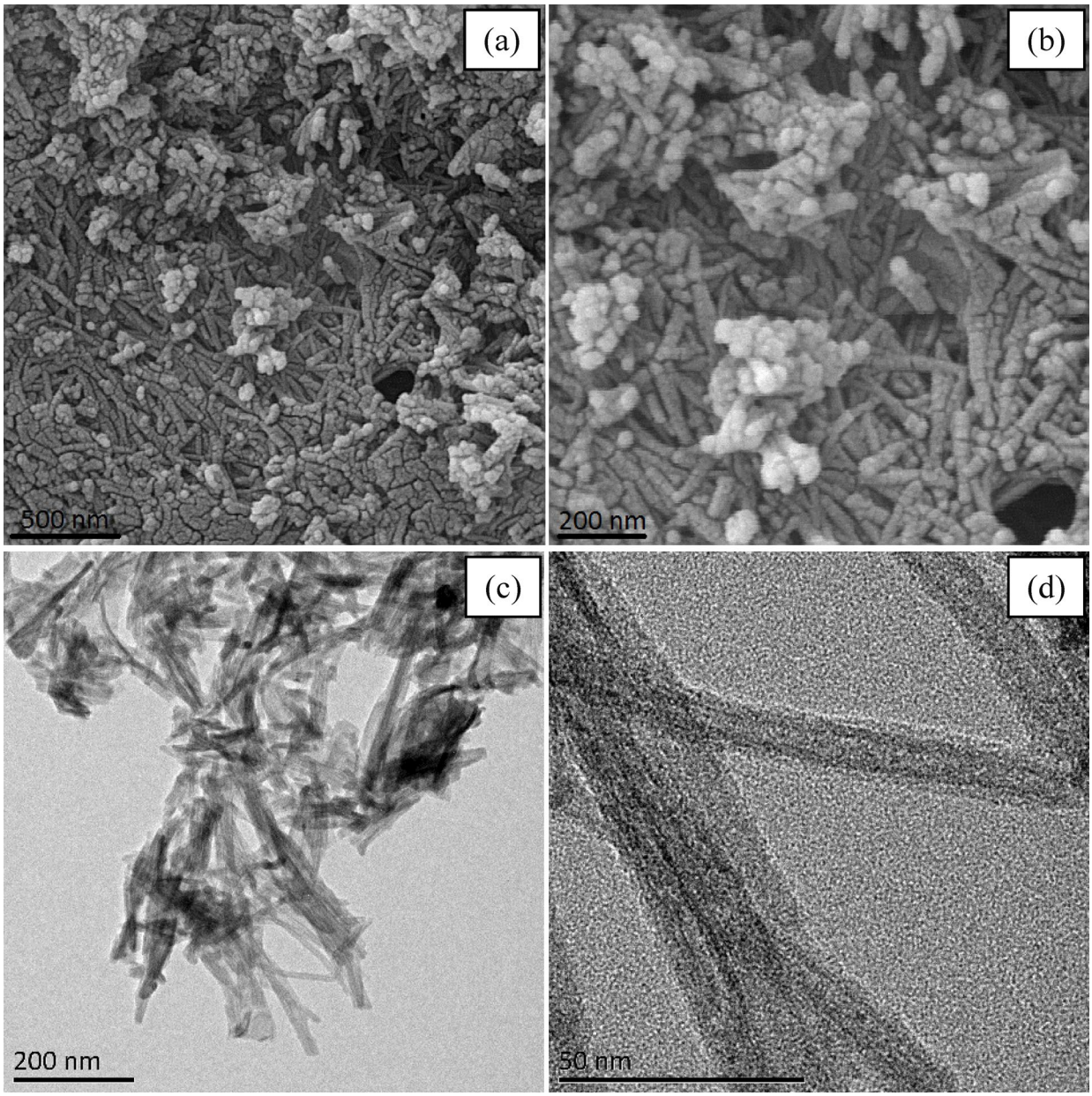

Fig. 3. (**a**, **b**) FE-SEM and (**c**, **d**) TEM images of TNTs@Cu(II)-SB, and EDX spectra of (**e**) TNTs, (**f**) TNTs@APTES, and (**g**) TNTs@Cu(II)-SB.

on TNTs (TNTs@Cu(II)-SB), the XRD pattern of TNTs does not changes significantly. This was anticipated as the functionalization of TNTs with APTES and synthesis of Cu(II) complex were carried out at relatively low temperatures which could not affect the crystal structure of TNTs[29,37].

Figure 2 shows the FT-IR spectra of bare TNTs, TNTs after synthesis of Cu(II)-SB complex, and the pure complex. The spectrum of bare TNTs displays an intense band at 462 cm^{-1} and a broad band between 600 and 800 cm^{-1}, attributed to Ti–O–Ti and Ti–O groups[39]. After complex formation, these bands intensify and broaden due to overlap with Cu–O and Cu–N stretching vibrations in the same region[40]. Besides, a distinct band at 1122 cm^{-1} and a shoulder at 1031 cm^{-1} can be observed at FT-IR spectrum of TNTs@Cu(II)-SB, which are ascribed to the Si–O and Si–O–Si groups of APTES, confirming its successful grafting onto TNTs[41,42]. The other bands appeared at 1258, 1331, 1445, 1545, and 1618 cm^{-1} can be assigned to the vibration of Ph–O, C–N stretching in amines, asymmetric bending of C–H, C = C aromatic, and vibration of C = N bonds in Schiff base, respectively[42–45]. As can be seen, these bands show slight shifts compared to those in the pure Schiff base complex. It is worth noting that the FT-IR spectrum of bare TNTs shows bands at 1382, 1457, and 1638 cm^{-1}, attributed to the bending vibrations of CH_3, CH_2, and N–H groups from residual SDS, respectively[46]. The presence of these bands, which can overlap with those of the Schiff base complex in these regions, indicates that SDS was not completely removed during washing. The FTIR spectra of all samples show two weak bands at about 2864 and 2921 cm^{-1} due to the symmetric and asymmetric stretching of aliphatic C–H[42,43]. Furthermore, the

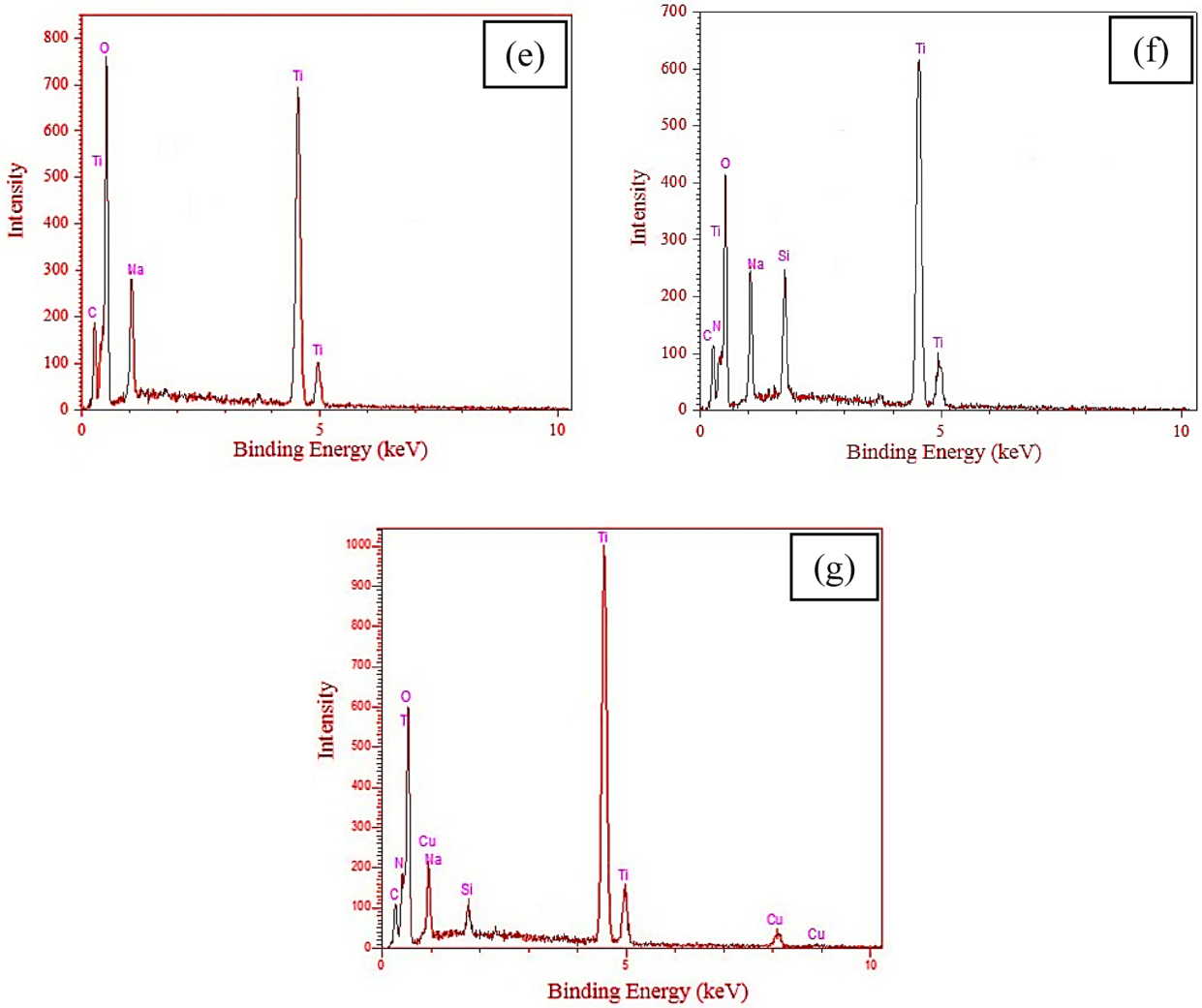

Fig. 3. (continued)

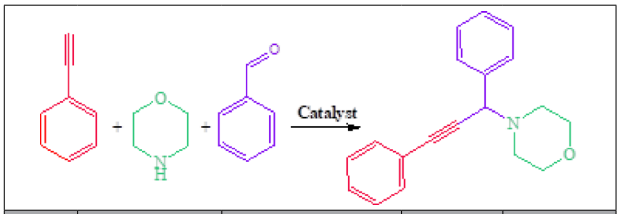

Entry	Catalyst (mg)	Temperature (°C)	Time (h)	Yield (%)[b]
1	2	120	4	90
2	4	120	4	99
3	6	120	4	62
4	4	100	4	80
5	4	80	4	56
6	4	RT	4	6
7	4	120	3	78
8	4	120	2	85
9	4	120	1	92

Table 1. The results of the various parameters optimization in A^3 coupling reaction using TNTs@Cu(II)-SB catalyst[a]. [a]Reaction condition: phenylacetylene (0.5 mmol), morpholine (0.55 mmol) and benzaldehyde (0.55mmol). [b]Isolated yield.

Entry	Alkyne	Amine	Aldehyde	Product	Yield (%)[b]	TON	TOF(h^{-1})
1		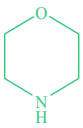	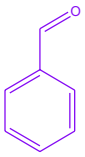	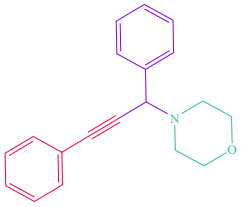	99	49	12.25
2	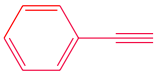	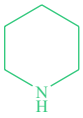	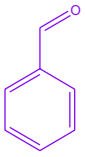	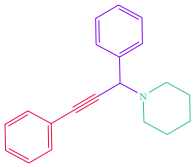	82	41	10.25
3		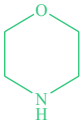	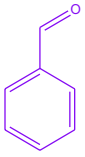	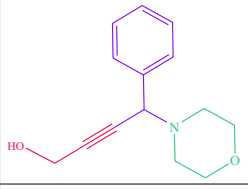	61	30.5	7.62
4		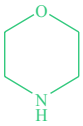	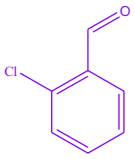	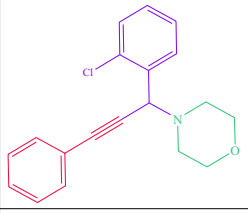	100	50	12.5
5	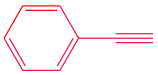	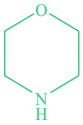	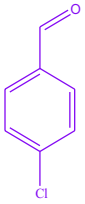	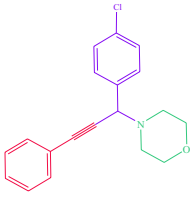	41	20.5	10.25
6	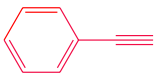	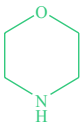	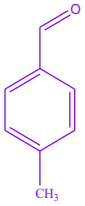	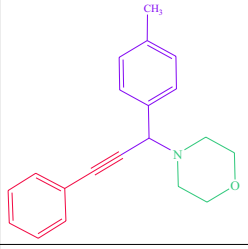	92	46	11.5
7		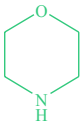	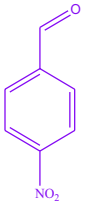	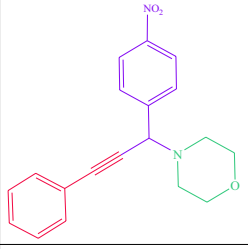	46	23	5.75
8	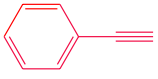	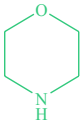	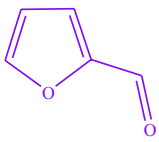	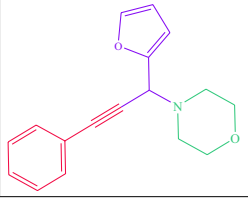	68	34	8.5

Table 2. A^3 coupling reaction of different substrates using TNTs@Cu(II)-SB catalyst[a]. [a]Reaction condition: alkyne (0.5 mmol), amine (0.55 mmol), aldehyde (0.55 mmol), and catalyst (4 mg) at 120 °C for 4 h. [b]Isolated yield.

Entry	Catalyst (Oxidation state of Cu)	Reaction conditions				Yield (%)	Refs.
		Catalyst loading	Temperature (°C)	Time (h)	Solvent		
1	Chit@CuI (Cu(I))	10 mg	140	0.75	-	83	[27]
2	ZSM-5@APTMS@(2-aminopyridine/terephthalaldehyde)@Cu-NPs (Cu(0))	25 mg	60	2	H_2O	98	[47]
3	[CuCl{2,5-bis(2-thienyl)−1-phenylphosphole}$_2$] (Cu(I))	0.1 mol % Cu	100	24	-	71	[48]
4	[Cu(N_2S_2)]Cl-Y (Cu(I))	3 mol %	70	12	Dichloroethane	90	[28]
5	Cu[(TS)PPh_3]Br (Cu(I))	20 mol %	80	5	Toluene	93	[23]
6	MCM-TSCuI (Cu(I))	3 mol %	80	4	Toluene	92	[49]
7	TNTs@Cu(II)-SB (Cu(II))	4 mg	120	4	-	99	This work

Table 3. Comparison of the catalytic activity of TNTs@Cu(II)-SB with some previously reported Cu-containing catalysts in A^3 coupling of phenylacetylene, morpholine, and benzaldehyde.

band related to the stretching vibration of O- H groups in adsorbed water molecules is observed at about 3357, 3414 and 3426 cm^{-1} for TNTs, Cu(II)-SB complex, and TNTs@Cu(II)-SB, respectively[41]. The FT-IR spectra confirm the formation of Cu(II)-Schiff base complex on APTES-grafted TiO_2 nanotubes.

The morphology of TNTs@Cu(II)-SB was assessed using FE-SEM and TEM images. FE-SEM images of sample (Fig. 3a and b) demonstrate randomly oriented rod-like nanostructures typical of TiO_2 nanotubes. Some aggregated nanoparticles can be observed in the FE-SEM images probably due to the incomplete transformation of TiO_2 nanoparticles to TNTs. TEM images of sample presented in Fig. 3c-d show that hallow tubes with lengths of several hundreds of nanometers and average diameter of ~8–13 nm were formed during the hydrothermal treatment of TiO_2 nanoparticles in concentrated NaOH.

The elemental analysis was performed to confirm the grafting of APTES and synthesis of Cu(II)-Schiff base complex on TNTs. According to EDX spectra (Fig. 3e-g), Ti and O are present as the main elements in as-prepared TNTs. The appearance of peaks related to N and Si elements in EDX spectrum of APTES-grafted TNTs reveals the successful functionalization of TNTs. After synthesis of Cu(II)-Schiff base complex, new peaks corresponded to Cu element can be detected in the EDX spectrum.

A comparative XPS study of the TNTs@Cu(II)-SB catalyst before use (Sample A) and after use (Sample B) in the A^3-coupling reaction demonstrates its remarkable stability. The Cu 2p spectra of both samples show nearly identical peaks at 934.7 eV (Cu $2p_{3/2}$) and 954.6 eV (Cu $2p_{1/2}$), with well-preserved shake-up satellite features in both Sample A and Sample B. This clearly confirms that the Cu(II) oxidation state remains intact throughout the catalytic process.

The Ti 2p spectra of Sample A (before use) and Sample B (after use) further demonstrate the structural stability of the catalyst support. The peaks corresponding to Ti $2p_{3/2}$ at 458.7 eV and Ti $2p_{1/2}$ at 464.4 eV show no significant changes in either sample, indicating complete preservation of the TiO_2 structure during the reaction.

Furthermore, the O 1 s spectra in both Sample A and Sample B show no notable changes. The lattice oxygen peak at 530.0 eV and surface species peak at 531.5 eV are well maintained in both samples.

The perfect match between Sample A (before use) and Sample B (after use) across all elemental spectra provides strong evidence for the structural stability of the catalyst and preservation of its heterogeneous nature. Therefore, we can conclude that the slight decrease in catalytic activity over multiple cycles is not due to chemical degradation, but rather to physical loss of some catalyst during the recovery and washing processes.

Catalytic studies

Considering the demonstrated catalytic potential of Cu(I)- and Cu(II)-Schiff base complexes in A^3 coupling reactions, we aimed to evaluate the performance of synthesized TNTs@Cu(II)-SB for this transformation. In this regard, phenylacetylene, morpholine, and benzaldehyde have been selected as model substrates, and key reaction parameters, including the amount of catalyst, reaction time, and temperature were optimized to establish efficient conditions for the three-component coupling process. The results are summarized in Table 1. Table 1 highlights the critical role of catalyst loading in optimizing product yield. Increasing the TNTs@Cu(II)-SB catalyst amount from 2 mg to 4 mg enhances the yield from 90% to 99% (entries 1–2), indicating enhanced catalytic efficiency at moderate loadings. However, a sharp decline in product yield to 62% occurs using 6 mg of catalyst (entry 3), which underscores the importance of balancing catalyst quantity for optimal performance. On the other hand, there is a direct correlation between the reaction temperature and product yield. The yield is negligible at room temperature (RT, entry 6), while it gradually increases with increasing temperature and almost complete conversion (99%) is achieved at 120 °C (entries 2, 4 & 5). In addition, the results reveal a nonlinear dependence of product yield on reaction time. The yield reaches 92% within the first hour but decreases to 85% and 78% by increasing the reaction time to 2 h and 3 h, respectively (entries 7–9). Notably, extending the reaction time to 4 h unexpectedly restores the yield to 99% (entry 2). According to the results, a reaction time of 4 h, a catalyst amount of 4 mg, and a temperature of 120 °C are suggested as the optimal operating conditions for the TNTs@

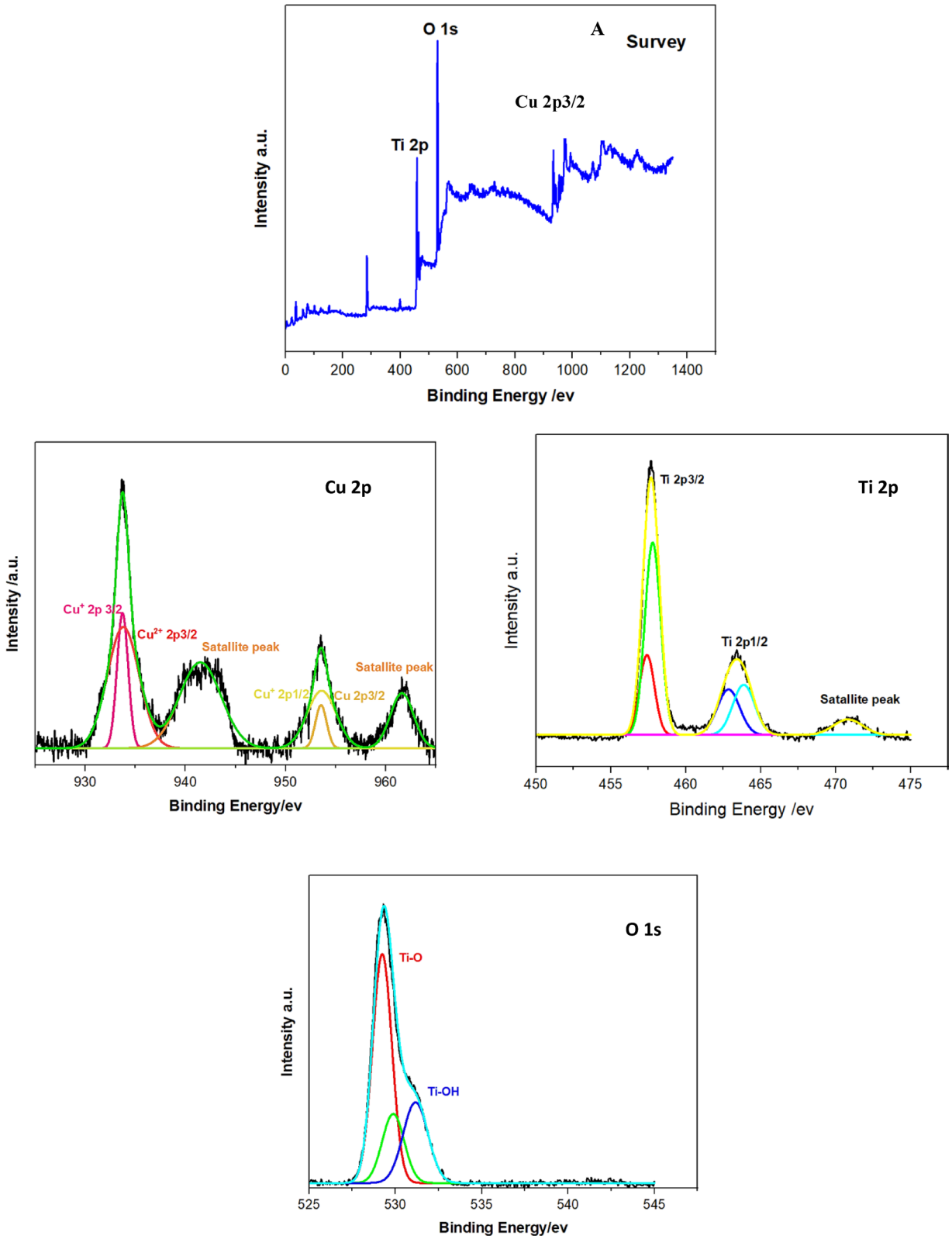

Fig. 4. XPS spectra of TNTs@Cu(II)-SB catalyst: (**A**) before use and (**B**) after use in A^3-coupling reaction.

Cu(II)-SB catalyst. The generality of TNTs@Cu(II)-SB catalyst was investigated using different substrates in A^3 coupling reaction under optimized conditions. As can be seen in Table 2, the product yield for different substrates varies in the range of 40% to 100%. Using piperidine as an amine instead of morpholine reduces the product yield by approximately 17% (entries 1 & 2). Similarly, product yield decreases by replacing phenylacetylene with

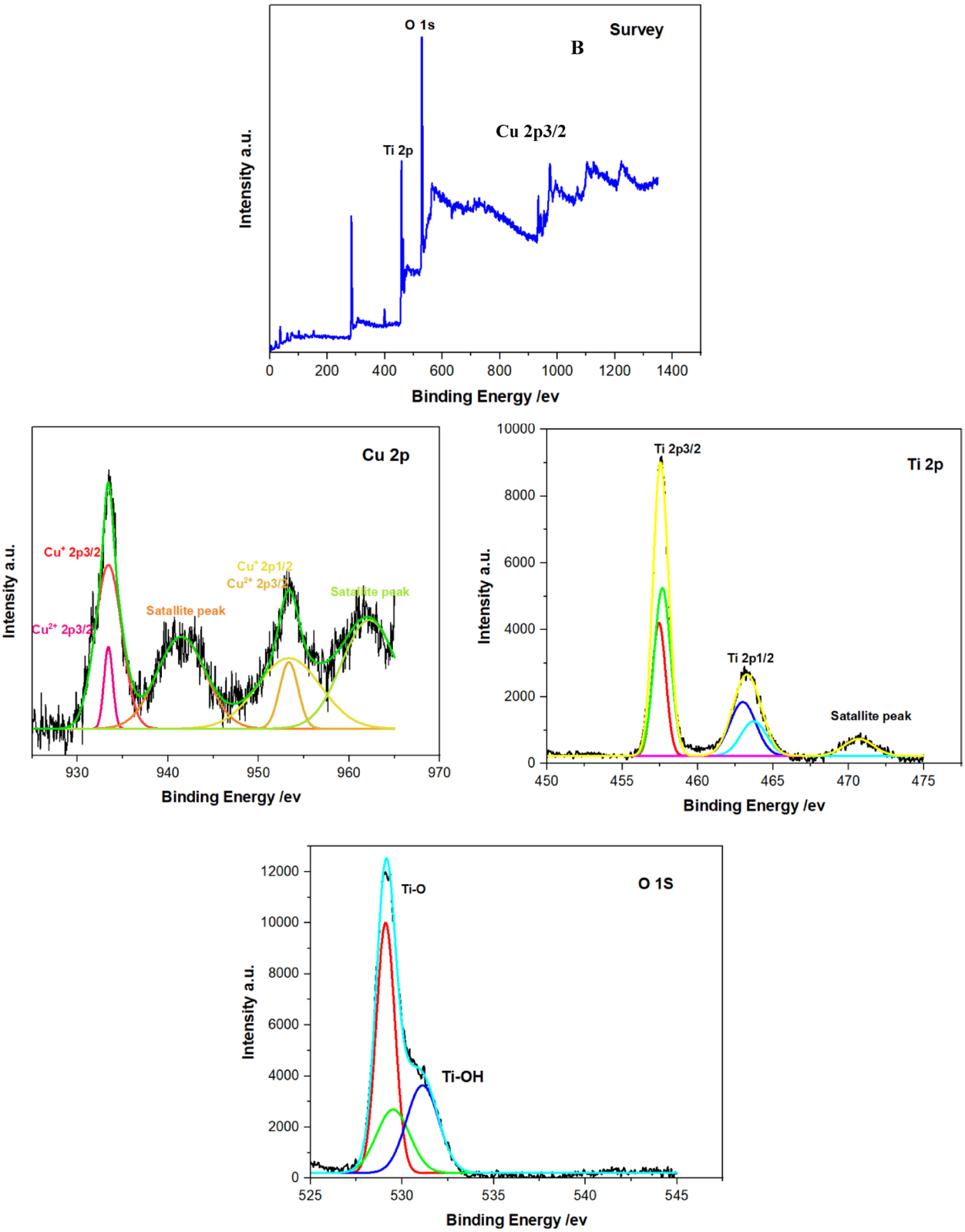

Fig. 4. (continued)

propargyl alcohol (entry 3). The results demonstrate that the best yield is obtained for 2-chlorobenzaldehyde (100%) among all the tested aldehydes (entries 4–8). It can be also concluded that 4-methylbenzaldehyde with an electron donating group in para position results in higher product yield in comparison to benzaldehydes having electron withdrawing groups in the same position (entries 5–7). Regarding the non-linear yield vs. time

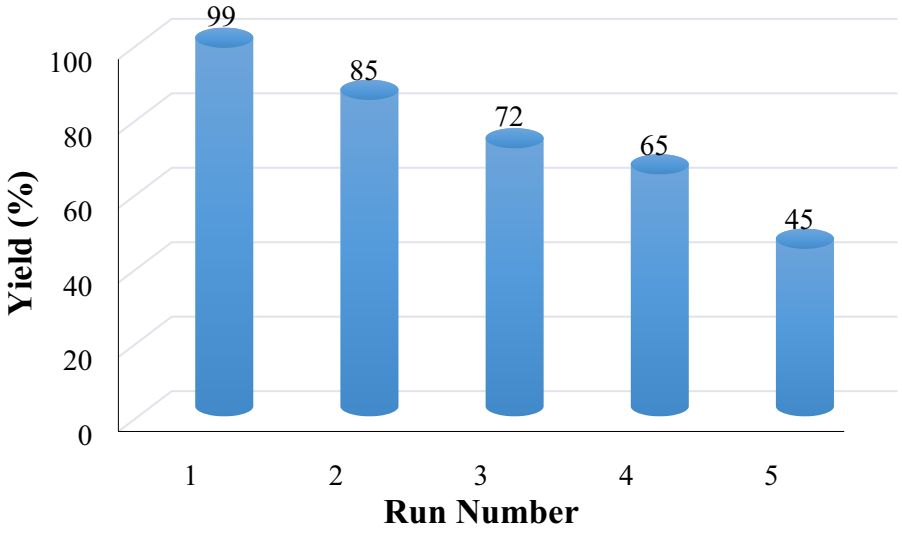

Fig. 5. Reusing TNTs@Cu(II)-SB catalyst in A^3 coupling of phenylacetylene, morpholine, and benzaldehyde.

trend observed in Table 1, this behavior may be attributed to several factors. Initially, the yield decreases possibly due to solvent evaporation, intermediate equilibrium, or catalyst deactivation. However, the yield recovers as the reaction proceeds, suggesting that catalyst reactivation or stabilization of reaction conditions may play a role in restoring the high yield. These points have been clarified to provide a comprehensive understanding of the reaction kinetics.

The generality of TNTs@Cu(II)-SB catalyst was investigated using different substrates in A^3 coupling reaction under optimized conditions. As can be seen in Table 2, the product yield for different substrates varies in the range of 40% to 100%. Using piperidine as an amine instead of morpholine reduces the product yield by approximately 17% (entries 1 & 2). Similarly, product yield decreases by replacing phenylacetylene with propargyl alcohol (entry 3). The results demonstrate that the best yield is obtained for 2-chlorobenzaldehyde (100%) among all the tested aldehydes (entries 4–8). It can be also concluded that 4-methylbenzaldehyde with an electron donating group in para position results in higher product yield in comparison to benzaldehydes having electron withdrawing groups in the same position (entries 5–7).

Table 3 compares the catalytic activity of synthesized TNTs@Cu(II)-SB with some previously reported Cu-containing catalysts in A^3 coupling of phenylacetylene, morpholine, and benzaldehyde. While direct comparison is challenging due to variations in reaction conditions, the synthesized catalyst exhibits significant catalytic activity. The desired product is obtained in high yield under solvent-free conditions with a low catalyst loading of 4 mg, reaching full conversion in just 4 h.

The reusability of TNTs@Cu(II)-SB catalyst in A^3 coupling of phenylacetylene, morpholine, and benzaldehyde was studied up to five runs. To this end, the catalyst was isolated after each run and washed with distilled water and ethyl ether. Then the dried catalyst was subjected to the next run under optimized conditions. The results presented in Figs. 4, 5 show that the product yield decreases somewhat after each run, probably due to the loss of catalyst during recovery process. Nevertheless, the catalyst can be reused up to 3 runs, offering a product yield of 72%.

The catalyst leaching was investigated by removing it from the reaction mixture of substrates (phenylacetylene, morpholine, and benzaldehyde) after the first 0.5 h. The reaction was then allowed to proceed for an additional 3.5 h in the absence of the catalyst. No product was obtained after this period, confirming the heterogeneous nature of the catalyst. Furthermore, AAS analysis of the reaction filtrate indicated that no copper species were present in the solution, confirming the strong immobilization of copper on the catalyst support.

Conclusion

In this work, TiO_2 nanotubes were synthesized by hydrothermal treatment of TiO_2 powder in concentrated sodium hydroxide solution and used as supports for preparation of Schiff base complexes of Cu(II). The presence of Cu(II)-Schiff base on TNTs was confirmed using different characterization techniques. A^3 coupling of phenylacetylene, morpholine, and benzaldehyde was chosen as a model reaction to evaluate the catalytic activity of synthesized material. An excellent yield of 99% was achieved using 4 mg of catalyst at 120 °C after 4 h. Using different substrates, good to excellent product yields were obtained which confirm the applicability of catalyst for most of substrates. The catalyst could be readily recovered by filtration and reused up to 3 runs with slight decrease in product yield. The leaching test did not rule out the possibility of catalyst leaching into the reaction medium.

Data availability

All data generated or analyzed during this study are included in this published article.

Received: 23 June 2025; Accepted: 18 December 2025
Published online: 07 January 2026

References

1. Jesin, I. & Nandi, G. C. Recent advances in the A3 coupling reactions and their applications. *Eur. J. Org. Chem.* **2019** (16), 2704–2720 (2019).
2. Volkova, Y., Baranin, S. & Zavarzin, I. A3 coupling reaction in the synthesis of heterocyclic compounds. *Adv. Synth. Catal.* **363** (1), 40–61 (2021).
3. Nasrollahzadeh, M. et al. A review on recent advances in the application of nanocatalysts in A3 coupling reactions. *Chem. Record*. **18** (10), 1409–1473 (2018).
4. Li, C. J. & Wei, C. Highly efficient Grignard-type Imine additions via C–H activation in water and under solvent-free conditions. *Chem. Commun.* **38**(3), 268–269 (2002).
5. McNally, J. J., Youngman, M. A. & Dax, S. L. Mannich reactions of resin-bound substrates: 2. A versatile three-component solid-phase organic synthesis methodology. *Tetrahedron Lett.* **39** (9), 967–970 (1998).
6. Wei, C. & Li, C. J. A highly efficient three-component coupling of aldehyde, alkyne, and amines via C – H activation catalyzed by gold in water. *J. Am. Chem. Soc.* **125** (32), 9584–9585 (2003).
7. Wei, C., Li, Z. & Li, C. J. The first silver-catalyzed three-component coupling of aldehyde, alkyne, and amine. *Org. Lett.* **5** (23), 4473–4475 (2003).
8. Samai, S., Nandi, G. C. & Singh, M. An efficient and facile one-pot synthesis of propargylamines by three-component coupling of aldehydes, amines, and alkynes via C–H activation catalyzed by NiCl2. *Tetrahedron Lett.* **51** (42), 5555–5558 (2010).
9. Li, P., Zhang, Y. & Wang, L. Iron-catalyzed ligand-free three-component coupling reactions of aldehydes, terminal alkynes, and amines. *Chemistry–A Eur. J.* **15** (9), 2045–2049 (2009).
10. Trang, T. T. T., Ermolat'ev, D. S. & Van der Eycken, E. V. Facile and diverse microwave-assisted synthesis of secondary propargylamines in water using CuCl/CuCl 2. *RSC Adv.* **5** (37), 28921–28924 (2015).
11. Yamamoto, Y. et al. Domino coupling relay approach to polycyclic pyrrole-2-carboxylates. *J. Am. Chem. Soc.* **127** (31), 10804–10805 (2005).
12. Beillard, A. et al. A3-Coupling reaction and [Ag (IPr) 2] PF6: a successful couple. *Eur. J. Org. Chem.* **2017** (31), 4642–4647 (2017).
13. Trose, M. et al. [Silver(I)(Pyridine-Containing Ligand)] complexes as unusual catalysts for A3-coupling reactions. *J. Org. Chem.* **79** (16), 7311–7320 (2014).
14. Rasheed, O. K. et al. The synthesis of group 10 and 11 metal complexes of 3, 6, 9-Trithia-1-(2, 6)-pyridinacyclodecaphane and their use in A3-Coupling reactions. *Eur. J. Org. Chem.* **2017** (35), 5252–5261 (2017).
15. Kidwai, M. et al. The first Au-nanoparticles catalyzed green synthesis of propargylamines via a three-component coupling reaction of aldehyde, alkyne and amine. *Green Chem.* **9** (7), 742–745 (2007).
16. Kidwai, M. et al. Copper-nanoparticle-catalyzed A3 coupling via CH activation. *Synlett* **2007** (10), 1581–1584 (2007).
17. Nasrollahzadeh, M., Sajadi, S. M. & Rostami-Vartooni, A. Green synthesis of CuO nanoparticles by aqueous extract of anthemis nobilis flowers and their catalytic activity for the A3 coupling reaction. *J. Colloid Interface Sci.* **459**, 183–188 (2015).
18. Sasikala, R. et al. Lanthanum loaded CuO nanoparticles: synthesis and characterization of a recyclable catalyst for the synthesis of 1, 4-disubstituted 1, 2, 3-triazoles and propargylamines. *RSC Adv.* **5** (70), 56507–56517 (2015).
19. Gajengi, A. L., Sasaki, T. & Bhanage, B. M. NiO nanoparticles catalyzed three component coupling reaction of aldehyde, amine and terminal alkynes. *Catal Commun.* **72**, 174–179 (2015).
20. Elhampour, A. & Nemati, F. Nano-Fe3O4@TiO2/Cu2O Core-shell composite: a convenient magnetic separable catalyst for A3 and KA2 coupling. *J. Chin. Chem. Soc.* **63** (8), 653–659 (2016).
21. Munshi, A. M. et al. Magnetically recoverable Fe3O4@ Au-coated nanoscale catalysts for the A 3-coupling reaction. *Dalton Trans.* **46** (16), 5133–5137 (2017).
22. Li, D. et al. Silver nanoparticles encapsulated by metal-organic-framework give the highest turnover frequencies of 105 h – 1 for three component reaction by microwave-assisted heating. *J. Catal.* **348**, 276–281 (2017).
23. Naeimi, H. & Moradian, M. Thioether-based copper (I) schiff base complex as a catalyst for a direct and asymmetric A3-coupling reaction. *Tetrahedron: Asymmetry*. **25** (5), 429–434 (2014).
24. Varyani, M., Khatri, P. K. & Jain, S. L. Amino acid ionic liquid bound copper schiff base catalyzed highly efficient three component A3-coupling reaction. *Catal Commun.* **77**, 113–117 (2016).
25. Agrahari, B. et al. Synthesis and crystal structures of salen-type Cu (ii) and Ni (ii) schiff base complexes: application in [3 + 2]-cycloaddition and A 3-coupling reactions. *New J. Chem.* **42** (16), 13754–13762 (2018).
26. Terra, J. C., Moores, A. & Moura, F. C. Amine-functionalized mesoporous silica as a support for on-demand release of copper in the A3-coupling reaction: ultralow concentration catalysis and confinement effect. *ACS Sustain. Chem. Eng.* **7** (9), 8696–8705 (2019).
27. Kaur, P. et al. Chitosan-supported copper as an efficient and recyclable heterogeneous catalyst for A3/decarboxylative A3-coupling reaction. *Tetrahedron Lett.* **59** (21), 1986–1991 (2018).
28. Naeimi, H. & Moradian, M. Encapsulation of copper (I)-Schiff base complex in NaY nanoporosity: an efficient and reusable catalyst in the synthesis of propargylamines via A3-coupling (aldehyde-amine-alkyne) reactions. *Appl. Catal. A*. **467**, 400–406 (2013).
29. Sun, Y. Y. et al. Hydrothermal synthesis of TiO2 nanotubes from one-dimensional TiO2 nanowires on flexible non-metallic substrate. *Ceram. Int.* **44** (3), 3501–3504 (2018).
30. Liu, S. et al. Synthesis of single-crystalline TiO2 nanotubes. *Chem. Mater.* **14** (3), 1391–1397 (2002).
31. Perera, S. D. et al. Hydrothermal synthesis of graphene-TiO2 nanotube composites with enhanced photocatalytic activity. *ACS Catal.* **2** (6), 949–956 (2012).
32. Zulfiqar, M., Chowdhury, S. & Omar, A. Hydrothermal synthesis of multiwalled TiO2 nanotubes and its photocatalytic activities for orange II removal. *Sep. Sci. Technol.* **53** (9), 1412–1422 (2018).
33. Khalaf, M. M. & Abd El-Lateef, H. M. Investigation of anti-corrosive potentials of Cu (II)–Schiff base complex assembled on magnetic Fe3O4, Fe3O4/TiO2 and Fe3O4/SiO2 nanocubes on carbon steel pipelines in 3.0 N HCl. *J. Mol. Liq.* **318**, 114251 (2020).
34. Kılınç, D. & Şahin, Ö. Effective TiO2 supported Cu-Complex catalyst in NaBH4 hydrolysis reaction to hydrogen generation. *Int. J. Hydrog. Energy*. **44** (34), 18858–18865 (2019).
35. Montaser, A. & Wassel, A. R. Al-Shaye'a, Synthesis, characterization and antimicrobial activity of schiff bases from Chitosan and salicylaldehyde/TiO2 nanocomposite membrane. *Int. J. Biol. Macromol.* **124**, 802–809 (2019).
36. Amoozadeh, A., Tabrizian, E. & Shahjoee, S. Nickel (II) schiff base complex supported on nano-titanium dioxide: A novel straightforward route for Preparation of supported schiff base complexes applying 2, 4-toluenediisocyanate. *Appl. Organomet. Chem.* **33** (9), e4956 (2019).

37. Jiang, F. et al. Effect of calcination temperature on the adsorption and photocatalytic activity of hydrothermally synthesized TiO2 nanotubes. *Appl. Surf. Sci.* **258** (18), 7188–7194 (2012).
38. Cui, L. et al. Facile microwave-assisted hydrothermal synthesis of TiO2 nanotubes. *Mater. Lett.* **75**, 175–178 (2012).
39. Becker, I., Hofmann, I. & Müller, F. A. Preparation of bioactive sodium titanate ceramics. *J. Eur. Ceram. Soc.* **27** (16), 4547–4553 (2007).
40. Abdel-Latif, S., Hassib, H. & Issa, Y. Studies on some salicylaldehyde schiff base derivatives and their complexes with cr (III), Mn (II), Fe (III), Ni (II) and Cu (II). *Spectrochim. Acta Part A Mol. Biomol. Spectrosc.* **67** (3–4), 950–957 (2007).
41. Begum, T. et al. Palladium-Schiff-base-silica framework as a robust and recyclable catalyst for Suzuki–Miyaura cross-coupling in aqueous media. *RSC Adv.* **5** (48), 38085–38092 (2015).
42. Meroni, D. et al. A close look at the structure of the TiO2-APTES interface in hybrid nanomaterials and its degradation pathway: an experimental and theoretical study. *J. Phys. Chem. C.* **121** (1), 430–440 (2017).
43. Vančo, J. et al. Synthesis, structural characterization, antiradical and antidiabetic activities of copper (II) and zinc (II) schiff base complexes derived from salicylaldehyde and β-alanine. *J. Inorg. Biochem.* **102** (4), 595–605 (2008).
44. Brnardić, I. et al. Sol–gel functionalization of sodium TiO2 nanotubes and nanoribbons with aminosilane molecules. *Ceram. Int.* **39** (8), 9459–9464 (2013).
45. Iftikhar, B. et al. Synthesis, characterization and biological assay of salicylaldehyde schiff base Cu (II) complexes and their precursors. *J. Mol. Struct.* **1155**, 337–348 (2018).
46. Piyamongkala, K., Mekasut, L. & Pongstabodee, S. Cutting fluid effluent removal by adsorption on Chitosan and SDS-modified Chitosan. *Macromol. Res.* **16** (6), 492–502 (2008).
47. Mohammadi, L. et al. Stabilization of copper nanoparticles onto the double Schiff-base-functionalized ZSM-5 for A 3 coupling reaction catalysis aimed under mild conditions. *RSC Adv.* **13** (7), 4843–4858 (2023).
48. Cammarata, J. R. et al. Single and double A3-coupling (aldehyde-amine-alkyne) reaction catalyzed by an air stable copper (I)-phosphole complex. *Tetrahedron Lett.* **58** (43), 4078–4081 (2017).
49. Naeimi, H. & Moradian, M. Copper (I)-N2S2-salen type complex covalently anchored onto MCM-41 silica: an efficient and reusable catalyst for the A3-coupling reaction toward propargylamines. *Appl. Organomet. Chem.* **27** (5), 300–306 (2013).

Acknowledgements

The authors gratefully acknowledge the financial and instrumental support provided by the Islamic Azad University, Science and Research Branch, and the University of Tabriz. The authors also acknowledge the assistance of OpenAI's ChatGPT in language editing and improving the clarity of the manuscript.

Author contributions

F.J. S., M. A. and A.A. K wrote the main manuscript text and F.J. S. and S.B. prepared Figs. 1, 2, 3 and 4; Tables 1, 2 and 3. All authors reviewed the manuscript.

Declarations

Competing interests

The authors declare no competing interests.

Ethics approval and consent to participate

This article does not contain any studies with human participants or animals performed by any of the authors.

Additional information

Supplementary Information The online version contains supplementary material available at https://doi.org/10.1038/s41598-025-33398-5.

Correspondence and requests for materials should be addressed to S.B. or M.A.